

# ANALYTICAL MODELS FOR COMPLEX ELECTROKINETIC PASSIVE MICROMIXERS

Yi Wang<sup>1</sup>, Qiao Lin<sup>1</sup> and Tamal Mukherjee<sup>2</sup>

<sup>1</sup>Dept. of Mechanical Engineering and <sup>2</sup>Dept. of Electrical & Computer Engineering,  
Carnegie Mellon University, 5000 Forbes Ave., Pittsburgh, PA 15213, U.S.A.

## Abstract

This paper presents composable and parameterized electrokinetic passive mixing models that are the first to simultaneously simulate both electric and concentration (partial mixing) networks at the system level and enable the design of efficient and compact mixers for integrated Micro-TAS. Model validity is verified by comparison to numerical data.

**Keywords:** composable system simulation, parameterized model, micromixer

## 1. Introduction

Micromixers are important components in Micro-TAS. Efficient mixing reduces analysis time, minimizes chip-area and improves process control. Currently, a majority of Micro-TAS use passive mixers that rely on molecular diffusion. In addition to their relatively simple fabrication processes, electrokinetic passive mixers are amenable to integration with electrophoretic analysis and can be easily controlled [1]. However, their efficient simulation and design continues to be a challenge and has not been extensively studied. Simplified equations [2] have been used to provide mixing length estimates that are often overly conservative, and modeling methods based on electric analogy assume complete mixing and may lead to extremely long channels [1]. In practice, however, complete mixing is often not necessary. In a microreactor, for example, after incoming reactants achieve a certain degree of premixing, product yield becomes reaction-limited. Attempts to further enhance mixing would not appreciably improve the yield, but lead to unnecessarily large chip-size and long mixing time. This paper presents analytical models to accurately capture electric current, flow ratio and concentration within the complex electrokinetic passive mixer and investigate the dependence of the mixing degree on system parameters, which can eventually speed up the design of efficient and geometrically compact mixers for integrated Micro-TAS.

## 2. Analytical Mixer Models

Consider a general mixing unit consisting of elemental combiners, splitters and mixing channels (length  $L$  and width  $w$ ) in Figure 1a [3]. An applied electric field  $E$  causes the buffer and species to move. Due to transversely uniform electrokinetic flow velocity, the concentration variation is independent of the depth-wise coordinate. In the combiner, arbitrary (rather than constant [3]) species concentrations from upstream channels are merged (Figure 1b). Its output concentration is found to be  $c_{out} = a_0s + b_0(1-s) + \sum d_n \cos(n\pi\eta)$  for  $n=1,2,3\dots$ , with  $d_n$  given by:

$$d_{n \neq 0} = \sum_{m=0}^{m=ns} \left\{ 2(-1)^n b_m (1-s) \left( \cos(F_2/2) \sin(F_1/2) / F_1 + \cos(F_1/2) \sin(F_2/2) / F_2 \right) + a_m s (f_1 \sin(f_2) + f_2 \sin(f_1)) / f_1 f_2 \right\} + \sum_{m=0}^{m=ns} (a_m s + b_m (-1)^m (1-s)) \quad (1)$$

where  $\eta=y/w$  is the normalized coordinate along channel width;  $a_m$  and  $b_m$  ( $m=0,1,2\dots$ ) are Fourier coefficients for concentrations from the input streams;  $s=I_1/(I_1+I_2)$  gives the interface position between the streams ( $I_1$  and  $I_2$  are currents through the streams);  $f_1=(m-ns)\pi$ ,  $f_2=(m+ns)\pi$ ,  $F_1=(m+n-ns)\pi$  and  $F_2=(m-n+ns)\pi$ . The Fourier coefficients  $h_n$  of the output concentration at the outlet of a mixing channel are given as

$$h_n = g_n e^{-\tau n^2 \pi^2} \quad (2)$$

where  $g_n$  are the input coefficients at the channel inlet, which is transferred from outlet of the upstream element, and  $\tau = LD/Uw^2$  ( $D$  and  $U$  are diffusivity and electrokinetic velocity of the species in the sample). For a splitter, the output coefficients are the same as the input ones, but the electric current is partitioned at a ratio depending on the downstream electric resistance.

### 3. Results and discussion

Results from analytical simulations of the mixer are shown in Figures 2-5. In Figure 2, analytical simulations of a cascade micromixer are compared with numerical data. Excellent agreement is found. We can see that at the combiner ( $com_3$  in Figure 2a), two streams with different concentration profiles are merged. Their interface position is around  $s=0.6$  (Figure 2b) determined by the currents through the streams. In Figure 3, electrokinetic focusing [4], which could be used to speed up mixing [5], is analytically simulated and compared to numerical data at two different focusing ratios  $\gamma$  (defined in Figure 3). A high  $\gamma$  can dramatically reduce the sample bandwidth supplied by the middle channel and accelerate the mixing. Figure 4 shows the analytical and numerical simulations of a multi-laminae (8 streams) electrokinetic mixer that also speeds up mixing by reducing widthwise diffusion distance [2]. It is found that at  $x=0.01L$ , mixing is achieved at 68% according to the mixing degree,  $Q = 1 - 2 \int_0^1 |c(\eta) - c_{avg}| d\eta$  ( $c_{avg}$  is the width-averaged concentration). Over  $0.3L < x < L$  (70% of the channel length),  $Q$  is only enhanced from 92% to 97%. This shows the usefulness of partial-mixing modelling in studying both mixer effectiveness and efficiency. Figure 5 shows the schematic of a split-and-recombine (SAR) mixer [6, 7] (Figure 1a) represented and simulated by our models (Figure 5a). Different from multi-laminae mixer in Figure 4, the SAR mixer performs multi-lamination within the mixer. The concentration distributions along  $\eta$  at the first four SAR units are illustrated in Figure 5b and multiple splitting of the species layers is clearly observed, which contributes to a tremendous improvement in  $Q$  compared with a T mixer of the same length (Figure 5c). We can also see that the increase in  $Q$  is rapid through the first few SAR units and then becomes saturated as species homogeneity improves. Thus, a tradeoff exists between  $Q$  and mixer size, mixing time and system complexity.

### 4. Conclusions

Analytical models have been presented for efficient simulations of complex electrokinetic passive micromixers. The models have been verified by numerical simulation data, and are able to accurately capture the combined effects of mixer geometry, buffer-species properties and system-operation parameters on mixing efficiency.

### Acknowledgements

This research is sponsored by DARPA and Air Force Research Laboratory, Air Force Material Command, USAF, under grant number F30602-01-2-0587, and the NSF ITR program under award number CCR-0325344.

### References

- [1] Jacobson, S. C.; McKnight, T. E.; Ramsey, J. M., *Anal. Chem.*, **71**, 4455-4459, (1999)
- [2] Koch, M.; Chatelain, D.; Evans, A. G. R.; Brunnschweiler, A., *J. Micromech. Microeng.*, **8**, 123-126, (1998)
- [3] Branbjerg, J.; Gravesen, P.; Krog, J. P.; Nielsen, C. R. *Proc. MEMS'96*, 441-446, 1996.
- [4] Jacobson, S. C.; Ramsey, J. M., *Anal. Chem.*, **69**, 3212-3217, (1997)
- [5] Knight, J. B.; Vishwanath, A.; Brody, J. P.; Austin, R. H., *Physical Review Letters*, **80**, 3863-3866, (1998)
- [6] Schwesinger, N.; Frank, T.; Wurmus, H., *J. Micromech. and Microeng.*, **6**, 99-102, (1996)
- [7] Schonfeld, F.; Hessel, V.; Hofmann, C., *Lab on a Chip*, **4**, 65-69, (2004)

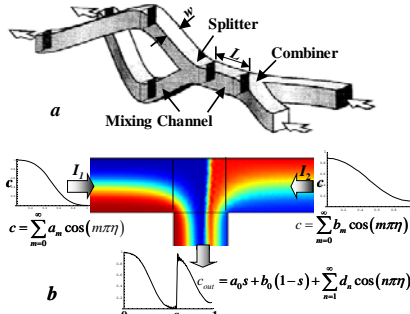


**Figure 1.** Geometry of the elements in a general mixer [3] (a) and modelling principle of the combiner (b).

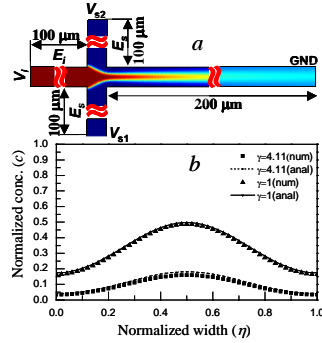


**Figure 3.** Concentration comparison of numerical data (a) with simulation using analytical model (b).  $D=1 \times 10^{-10} \text{ m}^2/\text{s}$ ,  $\mu=6 \times 10^{-8} \text{ m}^2/(\text{Vs})$ ,  $w=10 \mu\text{m}$ ,  $V_i=25 \text{ V}$ . Focusing ratio  $\gamma=E_s/E_i$ . For  $\gamma=4.11$ ,  $V_{s1}=V_{s2}=29 \text{ V}$  and for  $\gamma=1$ ,  $V_{s1}=V_{s2}=25 \text{ V}$ .

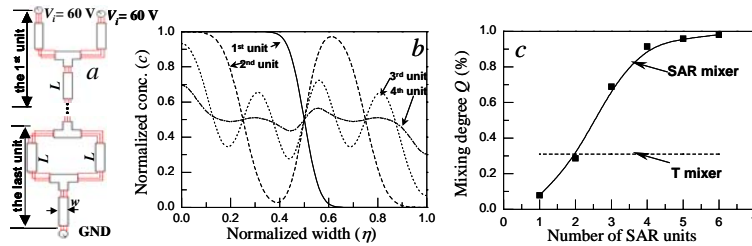


**Figure 5.** Analytical simulation results of SAR mixer. (a) composition of a SAR mixer. (b) concentration after the 1st, 2nd, 3rd and 4th SAR units. (c) The mixing degree  $Q$  after individual SAR unit, compared with T mixer. Properties are same to Figure 2, and  $L=800 \mu\text{m}$ ,  $w=200 \mu\text{m}$ .

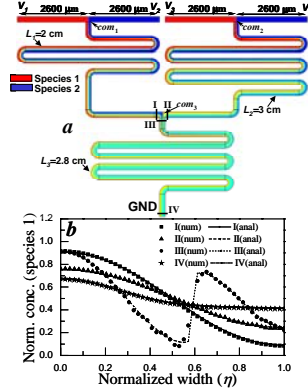


**Figure 2.** Concentration comparison of numerical data (a) with simulation using analytical model (b) (on species 1) at different positions (I, II, III and IV).  $w=200 \mu\text{m}$ ,  $D=2 \times 10^{-11} \text{ m}^2/\text{s}$ , mobility  $\mu=2 \times 10^{-8} \text{ m}^2/(\text{Vs})$ ,  $V_1=V_2=V_3=V_4=800 \text{ V}$ .

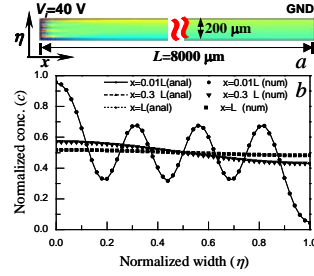


**Figure 4.** Concentration comparison of numerical data (a) with analytical results (b).  $D=1 \times 10^{-10} \text{ m}^2/\text{s}$ ,  $\mu=2 \times 10^{-8} \text{ m}^2/(\text{Vs})$ .